Experimental investigation of the effect of defects in Automated Fibre Placement produced composite laminates

Wilhelm Woigk[a,b], Stephen R. Hallett[a], Mike I. Jones[a], Moritz Kuhtz[b], Andreas Hornig[b], Maik Gude[b]

[a] *Advanced Composites Collaboration for Innovation & Science (ACCIS), University of Bristol, University Walk, Bristol BS8 1TR, UK*

[b] *Technische Universität Dresden, Institute of Lightweight Engineering and Polymer Technology (ILK), Holbeinstr. 3, 01307 Dresden, Germany*

Abstract

Automated composite manufacturing processes such as Automated Tape Laying (ATL) and Automated Fibre Placement (AFP) are effective methods to produce high quality, lightweight parts. Typically, preimpregnated fibres or tapes are laid side-by-side onto a tooling surface to generate the composite preform. Although these two main technologies are widely used to produce large composite components, inconsistencies such as overlapping tapes or gaps between adjacent tapes may occur during the manufacturing. Within this study, the effect of gaps and overlaps, so-called defects, has been investigated experimentally. Tensile and compressive testing has been carried out on specimens with a quasi-isotropic, symmetric layup into which artificial defects in various defined formations were introduced. Of particular interest were the strength knockdown factors and changes in the failure mode.

Keywords: A. Automated fibre placement, B. Defects, C. Fibre misalignment, D. Delamination

1. Introduction

Conventional hand lay-up techniques are strongly confined by the requirement of a manual operator during the manufacturing process. Furthermore, the size of the structure is limited by the worker's reach. In terms of these two aspects, it is obvious that the production of even small composite parts is time-consuming and becomes more uneconomical for greater production numbers. Thus automation is required in most industrial fields to increase the productivity as well as the structures' size [1].

In the area of composite manufacturing two main technologies have been established: Automated Fibre Placement (AFP) and Automated Tape Laying (ATL). These technologies are being employed today to manufacture advanced composite laminates from unidirectional prepregs. Both techniques are fairly similar to each other. ATL is able to place wide unidirectional prepreg tapes onto a tooling surface with automatic removal of the ply backing. AFP, in contrast, uses a band of narrow strips or tows of prepreg material. These strips are aligned in the layup head and can be cut individually if desired. Finally, the strips are layed down adjacent to each other [2]. By using one of these techniques large composite parts can be produced.

However, despite the high productivity and the ability to manufacture large parts, limitations in the AFP process can be identified. One of the limitations is the occurrence of defects during the layup process. These defects can either appear randomly or recurrently. The frequency of the occurrence depends on the complexity of the part and processing parameters such as tow width, layup speed and, if applied, tow steering. Steering induced defects such as tow buckling, tow pull-up and tow misalignment may occur if the steering radius is too small [2]. In general, defects cause discontinuities in the layup. Such discontinuities are characterised by a distortion of the fibre paths with unwanted fibre terminations. At the ends of the fibres, stress concentrations are likely to arise which significantly influences the mechanical performance of the composite.

Many authors have studied the effect of defects in the past in order to better understand and predict the influence of ply discontinuities that can for example occur in the manufacturing process. Sawicki and Minguet [3] studied the influence of gaps and overlaps on the compressive strength of composite laminates. They conducted their investigation with the background of the AFP techniques that are used in the fabrication of aircraft wings and fuselage skins. They carried out tests with up to 5 mm thick specimens, which contained defects with different widths from 0.76 mm (0.03 in) to 2.54 mm (0.10 in). The specimens had integrated defects only in the 90° off-axis plies in order to cause the most severe out-of-plane wrinkling in the adjacent, load-bearing 0° plies. It was found that a relatively sharp decrease in strength occurs when smaller gaps/overlaps are present. By increasing the defect width up to 2.54 mm, the reduction in strength is only slightly higher. The recorded strength knockdowns were approximately 8–13 %. Turoski [4] carried out experimental and numerical studies on the effects of manufacturing defects on carbon-epoxy composite strength. Gaps with different sizes and in certain distributions were introduced in composites during the manufacturing. Experiments on waisted unnotched and open hole specimens in both tension and compression were conducted. A maximum knockdown in the ultimate tensile strength (unnotched specimens) of slightly more than 15 % has been recorded. This knockdown was observed in the mean strength on specimens with "3 gaps". For the same specimen configuration ("3 gaps"), a knockdown of less than 10 % was recorded in compression. Croft et al. [5] carried out experiments on single gap, overlap and half gap/overlap specimens in tension and compression. They observed a negligible decrease of the ultimate strength for the gap containing specimens and even an increase for the specimens with overlaps (obtained for both tension and compression). The unexpected property rise for the overlap specimens is not well explained as it is claimed that it has been caused by an area calculation error. Li et al. [6] developed finite element meshing tools to effectively integrate defects in the layup. They modelled the out-of-plane waviness and ply thickness variations caused by gaps and overlaps and predicted the strength knockdowns for various defect combinations. Lan et al. studied experimentally the effect of isolated gaps and overlaps in various defect sizes on the tensile [7], in-plane shear and compressive [8] properties. They confirmed results reported by Li et al. [6] that defects in composites have a much smaller influence on the mechanical properties when a caul plate

was used during laminate curing. The caul plate reduced significantly thickness variations and allows for resin flow. Compared to the reference composites, strength knockdown factors of less than 10, 5 and 12% were reported for tension, in-plane shear and compression, respectively.

That defects such as gaps and overlaps can cause fibre misalignments, particularly in the out-of-plane direction (thickness direction of the laminate), has been shown by different authors [3, 5, 9]. Hsiao and Daniel [10] earlier studied the effect of fibre waviness on the mechanical (compressive) properties of fibre composites. However, the waviness in their specimens was not induced by defects but introduced by a uniform waviness in a tape-winding process. They found that fibre misalignments cause interlaminar shear and through-thickness normal stresses. Due to the presence of such stresses a delamination failure in composites is most likely. After delamination has occurred, a lower fibre support is provided by the matrix. This makes the specimen even more susceptible to global buckling because of the reduced thickness of now individually acting laminae compared with the initial component.

In general, the term defect may be used to describe an enormous range of possible phenomena in structures as discussed above [11, 12]. In this research, only manufacturing related artefacts are described as defects. Two types of defects that may arise during processing have been identified. Ideally, adjacent tows should be laid down precisely side-by-side onto the surface of a mould. However, when the tooling geometry becomes more complex, gaps between the tows may be created (Figure 1a) or the tows overlap slightly (Figure 1b). These two types of defects, which have been also studied previously by other authors [5, 7, 8], were selected for isolated (only gaps or overlaps) and combined (gaps and overlaps) studies to investigate their effect on the mechanical performance.

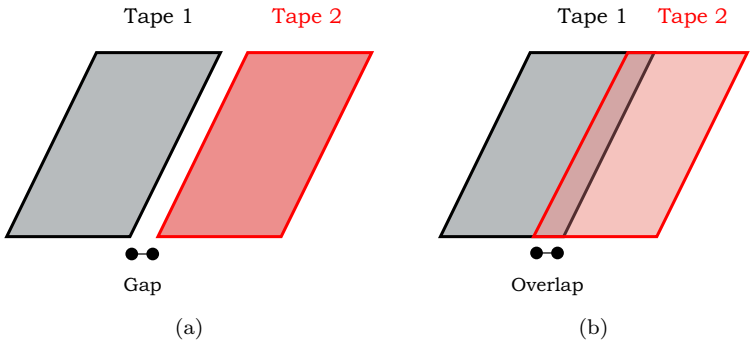

Figure 1: Schematic definition of (a) Gap and (b) Overlap defect types between adjoining tapes, adapted from [6]

It should be noted that due to the AFP manufacturing method of laying down unidirectional material, the local defect orientation is inherently parallel to the fibre direction. This aspect is important and so was taken into account in the manual manufacturing process of the defect containing composites. In this context, a very high number of defect combinations can be integrated. In this study, constant defect size

and stagger distance, both 2 mm, were considered. The defects were integrated into the off-axis plies, i.e. ±45 and 90° plies. Figure 2 shows a possible defect distribution within a layup. In the side-on schematic on the left side, the defects are illustrated as rectangles and may be either gaps or overlaps. The close-up view on the right side depicts the paths of three defects through each ply of one sub-laminate.

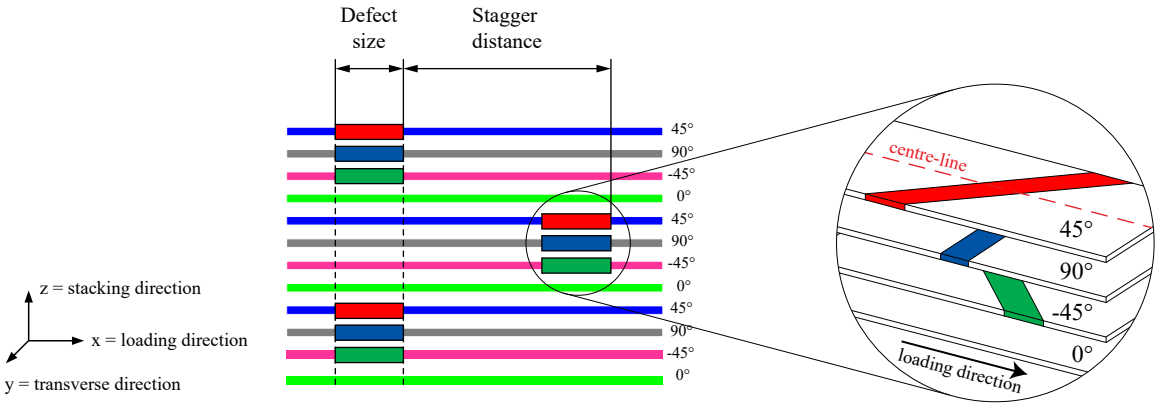

Figure 2: Layup of a defect containing laminate. The left view shows the side-on schematic through the specimen centre-line, illustrating the defects as coloured rectangles and defining the parameters "defect size" and "stagger distance". The close-up view on the right shows the paths of the defects through one sub-laminate.

When laying down the tows onto a surface with a complex shape, a defect distribution may be very repetitive due to automation, or it may be highly random. Therefore, it is important to understand the influences and the driving mechanisms of separate and combined defects, which is thus far not well understood. In the study presented here, pristine test specimens, along with samples that have artificially introduced defects, have been tested in tension and compression. The averaged ultimate strength values and the failure behaviour were analysed and compared. The aim was to develop a defect configuration with a sufficiently high severity to study effects of gaps and overlaps defects on both the failure strength and failure mode. It should be noted that the presented effects on properties and failure sequences are only valid for the defect formations presented in this paper.

2. Experimental procedure

2.1. Defect types selection

Several defect configurations were developed in addition to pristine specimens. The gap and overlap formations are illustrated schematically in Figure 3. In this figure, the red and yellow rectangles illustrate gap and overlap defects, respectively. In the first step, the gaps and overlaps were considered independently and in an aligned configuration (see "Gaps" and "Overlaps" specimens in Figure 3). To obtain a higher

induced out-of-plane fibre misalignment severity, a stagger was introduced to the defect configuration (see "Staggered Gaps") and subsequently a staggered gap and overlap combination (see "Gaps & Overlaps").

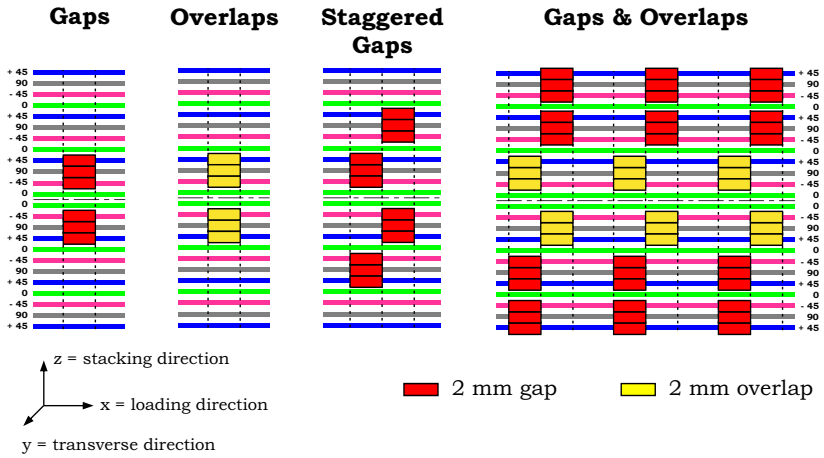

Figure 3: Overview of defect configurations, shown are the middle-cross-sections

Before specimens of the defect configurations, introduced in Figure 3, were prepared for testing, typical sample cross sections, in which all defects intersect, were inspected via cut up and optical microscopy (Figure 4). The micrographs depict the structural changes within the layup when defects are present. It can be seen that gaps allow for the creation of resin pockets and space for the innermost layers to deflect towards the centre line. Contrary, the overlaps force the layers to bend in the direction of the laminate surfaces.

2.2. Manufacturing techniques

The laminates were manufactured through manual layup of unidirectional carbon fibre prepreg plies (IM7/8552 by Hexcel). Although the hand layup has a low productivity and might not be entirely representative for automated fibre laying processes, it allows one to work with a good accuracy to isolate single or controlled occurrences of defects in the specimen gauge sections to mimic actual defects in the AFP process. The selection of defect type and severity was inspired by industrial observations. The hand layup technique becomes particularly suitable when staggered defects need to be precisely placed. The plies of different layers have been stacked in such manner that the final composites had a $[+45_2/90_2/-45_2/0_2]_{3S}$ quasi-isotropic layup. For each direction, two plies of the same orientation were doubled up before layup and were treated as a single, blocked ply of increased thickness. The ply thickness has significant influence on the failure mode and the failure strength of quasi-isotropic composites [13]. A nominal cured ply thickness of 0.25 mm was used to allow for delamination dominated failure. To design the crossing defects in the layup, the gaps and overlaps had to be integrated into the cutting layout. Therefore, ply related cutting paths were generated in

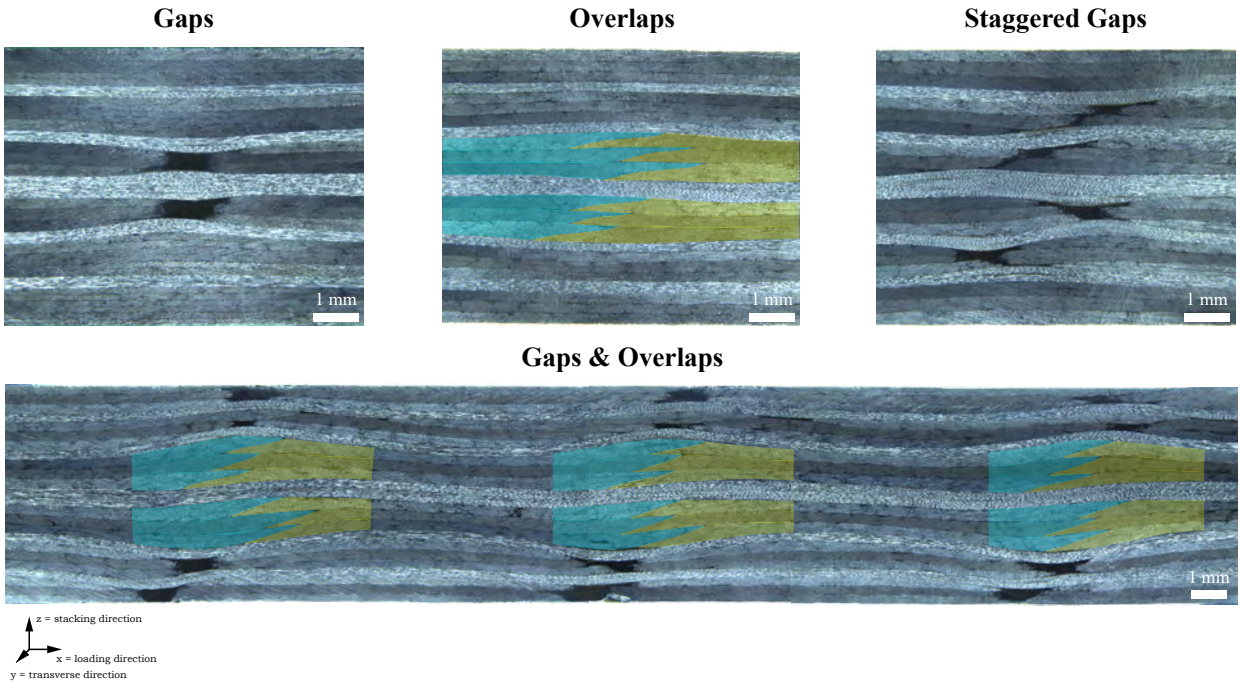

Figure 4: Microscopy images of the middle cross sections of the defect containing specimens revealing fibre misalignments caused by the gap and overlap defects. The gaps are present in form of resin pockets (black regions), whereas the overlaps are indicated by the transparent blue and yellow shapes

the Autodesk INVENTOR CAD software. The cutting of the plies was done by an automated ply cutting machine.

Figure 5 shows exemplary how 2 mm wide gaps were created during the layup process. Composite spacers with a width of 2 mm were used to separate plies within one layer (Figure 5a). In addition, woven strips that do not affect the composite's properties were placed at the edges of the panel (Figure 5b). These strips are visible after the composite curing, which allows for a accurate extraction of test specimens from the cured plate. Figure 5c further shows that 2 mm staggers can be precisely realised. Such staggers have been introduced into the defect configurations "Staggered Gaps" and "Gaps & Overlaps" (see schematics in Figure 3).

The prepreg stacks were cured in a laboratory autoclave, using a curing cycle for monolithic components in accordance with the manufacture's product data sheet [14]. The processing parameters during curing were recorded by thermocouples and pressure gauges. During the curing of the prepreg plates, a flat tooling base and 6 mm steel caul plates were used to achieve specimens with constant thickness and a flat surface on both sides.

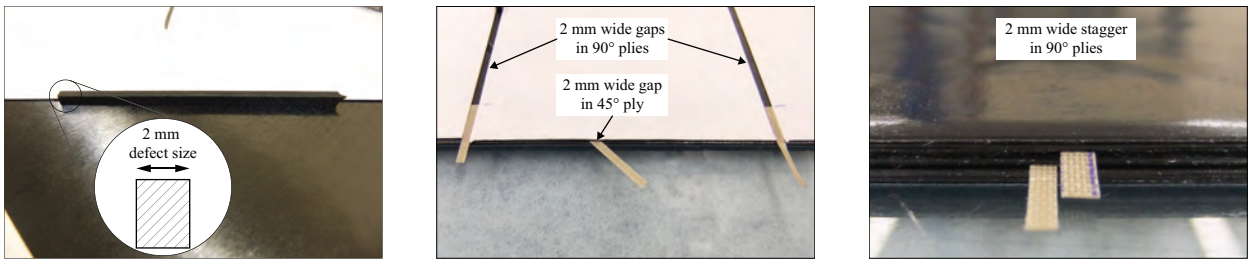

(a) (b) (c)

Figure 5: Gap manufacturing process; (a) Use of 2 mm wide spacer in placement of the broadgoods plies, (b) Achieved gaps in the plies and edge markers to better locate the defects after composite curing (white backing paper is visible on the ply upper surface) and (c) Specimen during the layup showing the introduction of precise staggers

2.3. Test methods and set-up

The effects of artificially integrated gaps and overlaps were experimentally studied via tension and compression tests. Both test methods were carried out at ambient temperature using a servo-hydraulic Instron^{TM}universal material testing machine with a 250 kN load cell.

The test specimen size was 250 mm x 30 mm and 116 mm x 30 mm for the tension and the compression test coupons, respectively. The thickness for both types was nominally 6 mm. Both sets of specimens had bonded on glass fibre-reinforced epoxy end tabs, acting as sample support in the clamping region, leading to a gauge length of 150 mm and 36 mm for the tension and compression specimens, respectively. The compression samples' gauge section was chosen to allow the cross-over defect zone to be entirely within the gauge section (see schematic in Figure 6).

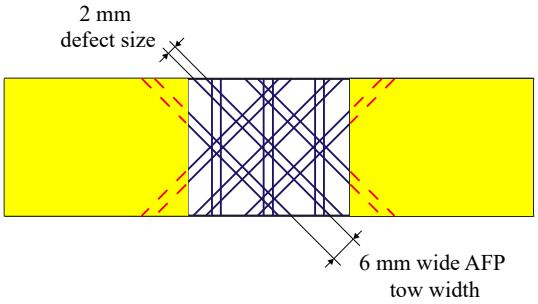

Figure 6: Top view schematic of the compression specimens of defect configuration "Gaps & Overlaps" with defect cross-over points within the gauge section, the red dashed lines indicate the defect path underneath the end tabs which are shown in yellow

The tensile tests were carried out in accordance with ASTM D3039. Samples were clamped in the testing machines grips with a clamping pressure of 6 bar to prevent slippage of the samples. The tensile load was applied with a displacement controlled rate of 0.5 $^{mm}/_{min}$. The compression specimens were tested

using the so-called Imperial College test method proposed by Haeberle and Matthews [15]. This method was favoured because of its ease in terms of jig handling along with a combined loosely clamped end and shear load introduction, which reduces premature specimen damage due to decreased stress concentrations [15, 16]. Because of the shorter gauge length of the compression specimens, a reduced constant loading rate of 0.25 $^{\mathrm{mm}}/_{\mathrm{min}}$ was used. The force and displacement data were recorded at a sampling rate of 10 Hz. Seven pristine samples and four specimens for each defect configuration were tested in tension. Akin, six pristine, "Gaps" and "Gaps &Overlaps" and five "Overlaps" and "Staggered Gaps" specimens were tested in compression. Because of the goal to test cross-over defects, meaning the integrated defects intersect in the centre of the specimen's gauge section, only a limited number of samples could be extracted from the laminates.

A Photron Fastcam SA1.1 high speed camera (HSC) equipped with a Nikon Micro-Nikkor 105 mm f2.8 type lense was used for both test methods to record the damage behaviour during the failure of the specimens. The focus of the camera was always set to one edge of the specimens. Although, the observed phenomena are not fully representative for the entire coupon because of edge effects, this high speed camera system allows for the analysis of relevant highly-dynamic failure mechanisms. In [13], it is pointed out that in test coupons initial failure is controlled by free edge delamination due to high interlaminar shear stresses as a result of limited specimen size. Since delamination can be induced by shear stresses associated with free edges, the chosen measurement set-up can detect initial delaminations. The frame rate of the HSC was set to 48'000 frames per second. This high frame rate comes slightly at the cost of image resolution. However, capturing images with a smaller time interval was preferred to gain a better insight into the failure behaviour.

3. Results and Discussion

The pristine and the defect containing specimens were tested in both tension and compression. The majority of the tests were conducted accompanied by high speed camera (HSC) recordings to analyse the failure mode, the location of damage initiation and potential changes due to the introduction of the different defects. Because of the capturing of the images at a high frame rate compared to the sampling rate of the load data, the difference in time between the frames are given in the individual frame series. The HSC series show the failure event and were thus recorded at less than 1 % below maximum stress. The very last image of each series was chosen to be $t = 0$.

The analyses of the tests are divided into the following sections:

- Failure Test Results - Tension (Strength and stiffness),
- High Speed Camera Analysis - Tension (Failure behaviour),
- Failure Test Results - Compression (Strength and stiffness),
- High Speed Camera Analysis - Compression (Failure behaviour).

3.1. Tensile testing

3.1.1. Strength and stiffness

The recorded stress-displacement curves of the tensile specimens are shown in Figure 7. Four curves per batch are illustrated, which are separated by an displacement offset of 1 mm to better distinguish the stress-displacement curves of each of the specimen configurations.

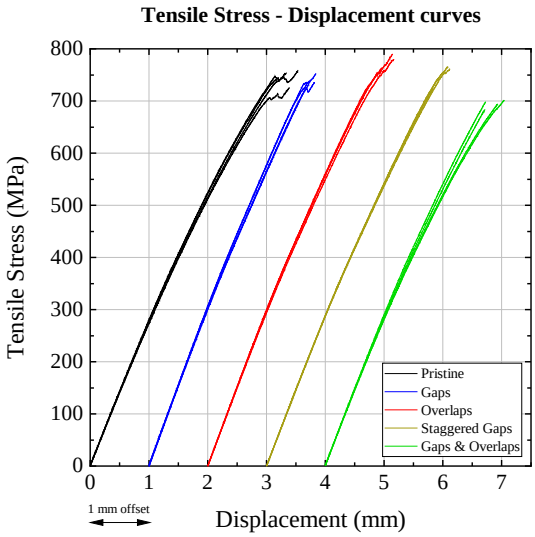

Figure 7: Tensile stress-displacement curves (horizontal offset added for a better visualisation)

It can be seen that all of the curves exhibit a similar slope in the lower displacement region. The slope relates to the stiffness of the samples. Although, the deformation in the sample gauge section was not explicitly measured, by for example using a clip-on extensometer, the tensile moduli, E_t, were calculated based on the crosshead displacement. Therefore, the strain range 0.05 – 0.25 % was used. The average of the measured moduli for the pristine and the defect configurations are reported in Table 1. The pristine specimens show the lowest tensile modulus, which could be a manufacturing related issue, for example a slightly misaligned specimen extraction from the composite. The moduli of the defect containing specimens decrease negligibly with increasing number of defects. A drop in the modulus when integrating severe defect formations was not expected. The defects should not have such a great influence on the mechanical performance within the small strain range in which the tensile modulus was calculated. However, at larger displacements, the deviation from the linear-elastic material behaviour is obvious and it is more pronounced for the specimens with a higher number of defects. In addition to the measurements, the equivalent laminate modulus in the longitudinal direction for the quasi-isotropic layup was calculated using classical laminate theory (CLT). The engineering constants for unidirectional IM7/8552 were taken from Lander et al. [17]. Two cases for the laminate analysis were considered, i.e. single ply and blocked ply thickness. For both

cases an in-plane isotropic modulus of 62 GPa was calculated. This, on one hand, proves that the elastic modulus is independent of the ply thickness and, on the other hand, that the CLT model predicts a good approximate stiffness.

The difference in the ultimate tensile failure strength can be also clearly seen in the stress-displacement diagram. In Table 1 the number of samples tested, n, the average ultimate tensile failure strength, $\bar{\sigma}_{t\,max}$, including its standard deviations, and the coefficients of variation for failure strength, CV, are summarised. In addition, this table depicts the relative change in ultimate tensile strength compared to the pristine properties (referred to as knockdown factors).

In order to determine the statistical significance of these knockdown factors, a non-parametric statistical test was carried out. A non-parametric tests is necessary to perform as a normal distribution cannot be assumed because of the low sample number. Therefore, a two-tailed Wilcoxon rank test with the null hypothesis of "zero median", i.e. no difference between two sets of data, and a level of significance of 0.05 was carried out. The P-values and the interpretation of the statistical tests are reported in Table 1. It should be noted that a statistical significance may be also caused by negative knockdown factors.

Table 1: Summary of *tensile* properties of pristine and defect specimens and results of statistical significance based on Student's t-test

Configuration	n	E_t (GPa)	$\bar{\sigma}_{t\,max}$ (MPa)	CV of $\bar{\sigma}_{t\,max}$ (%)	Knockdown factor for $\bar{\sigma}_{t\,max}$ (%)	P-value	Significant difference in strength
Pristine	7	69.8 ± 0.7	750 ± 12.5	1.90	–	–	–
Gaps	4	76.7 ± 0.3	740 ± 7.7	1.05	1.3	0.2303	no
Overlaps	4	75.7 ± 0.6	773 ± 13.4	1.73	-3	0.0242	yes
Staggered Gaps	4	72.9 ± 0.4	749 ± 19.4	2.59	0.2	0.98	no
Gaps & Overlaps	4	72.3 ± 0.8	694 ± 7.6	1.10	7.4	0.0061	yes

The pristine specimens reached an average failure stress value of 750 MPa. This measure correlates with values reported in the literature. For example, Wisnom et al. [18] measured a failure strength of 660 MPa for a 16 layer quasi-isotropic IM7/8552 layup with blocked plies. In K. Marlett [19], a tensile strength of 722 MPa for a single ply quasi-isotropic layup is reported.

The "Gaps" type specimens yielded an average strength value of 740 MPa, which is negligibly below the pristine property. The six gaps in the middle-most sub-laminates of the specimens have not had a significant influence on the ultimate tensile strength. The "Overlaps" specimens yielded the highest ultimate strength values among the various specimen types. Hence, the average stress value led to a negative knockdown factor compared with the pristine. It is assumed that the higher fibre volume content in the overlapped

regions adds sufficient integrity, enabling the specimens to bear the applied load, especially towards the end of each test. Another result that was not expected is the ultimate failure stress value of the "Staggered Gaps" configuration. The mean value varied just 1 MPa from the pristine, leading to a very little knockdown of 0.2 %. After developing and testing more severe defect formations, the "Gaps & Overlaps" configuration eventually depicted a significant knockdown in the averaged strength value. The significance of the "Gaps & Overlaps" knockdown was proven by the t-test. In addition, the average strength value is beyond the scatter of the other defect configurations and has itself an acceptably low standard deviation.

3.1.2. Failure behaviour

Almost every individual test was accompanied by high speed camera (HSC) recordings of one edge of the specimen. In this way, out-of-plane fibre misalignments and failure initiation could be observed. One representative series of HSC frames for each defect configuration and for the pristine case is shown. The frames are extracted prior to the failure event. Since the used frame rate is significantly higher compared to the load data acquisition rate, it can be assumed that the five images that are presented for every failure event are captured at less than 1 % below maximum load. In the analysis, similarities and differences in the damage development and final failure between the specimens of different defect configurations and within one configuration are discussed.

a) Pristine

Quasi-isotropic specimens with +45° or -45° surface plies exhibit matrix cracks in these plies relatively early in the loading process when loaded in tension. Furthermore, the cracked pieces have a tendency to peel off from the specimen (indicated by the yellow oval in Figure 8 (a)). The cracking event is clearly accompanied by an audible sound. These premature transverse matrix cracks that arose also in the 90° plies, were followed by delamination. As it is shown in frame (a) in Figure 8, delaminations occur at the weakest interfaces between off-axis plies of different fibre orientation, i.e. +45/90 and 90/-45 interface. This was also observed in the experimental work in Ref. [20] and Ref. [21]. Transverse matrix cracks arise relatively early in the 90° plies because of their relatively low strength in the loading direction. At those matrix cracks, high interlaminar shear stresses develop and thus delamination occurs. Furthermore, the transverse cracks allow the delamination to migrate between ply interfaces.

Although significant delaminations and large cracks were present, the load bearing 0° plies were still intact and no load drops were recorded. Upon further loading, fibre failure in one 0° ply occurred (see red oval in Figure 8 (b)) which led to sudden load shedding of the specimen. Figure 8 (c) is the first image of the catastrophic failure. This frame shows the fibre failures within the outer sub-laminates, whereas the 0° plies seem to be still intact at the point of specimen failure. Figure 8 (d) and (e) depict the failure event further.

The precise failure mode is uncertain and presumably a combination of both delamination and subsequent fibre failure. However, due to the large amount of premature ply separation, it can be classified as a delamination driven failure [22]. That means, according to the tensile test failure mode reported in the tensile test standard (ASTM D3039 [23]) the specimens failure can be classified as DGM (D: edge delamination, G: gage, M: middle) followed by XGM (X: explosion, G: gage, M: middle). It should be noted that this classification of the failure sequence is valid for all of the defect configurations tested. The differences in the damage progression and the failure mode is discussed in the respective paragraphs and compared in the discussion.

A leading explanation as to why the specimens failed by delamination is the amount of the blocked plies. The number of blocked plies has a significant influence on the failure mode. In the considered case, the number of blocked plies is 2 which leads to a nominal ply thickness of 0.25 mm. In Garrett and Bailey [24] it was found that the susceptibility to matrix cracks increases with an increase in ply thickness. This correlates with the test results reported by Wisnom and Hallett in [21, 22]. Consequently, the final failure of the specimens was preceded by transverse cracking and free edge controlled delaminations.

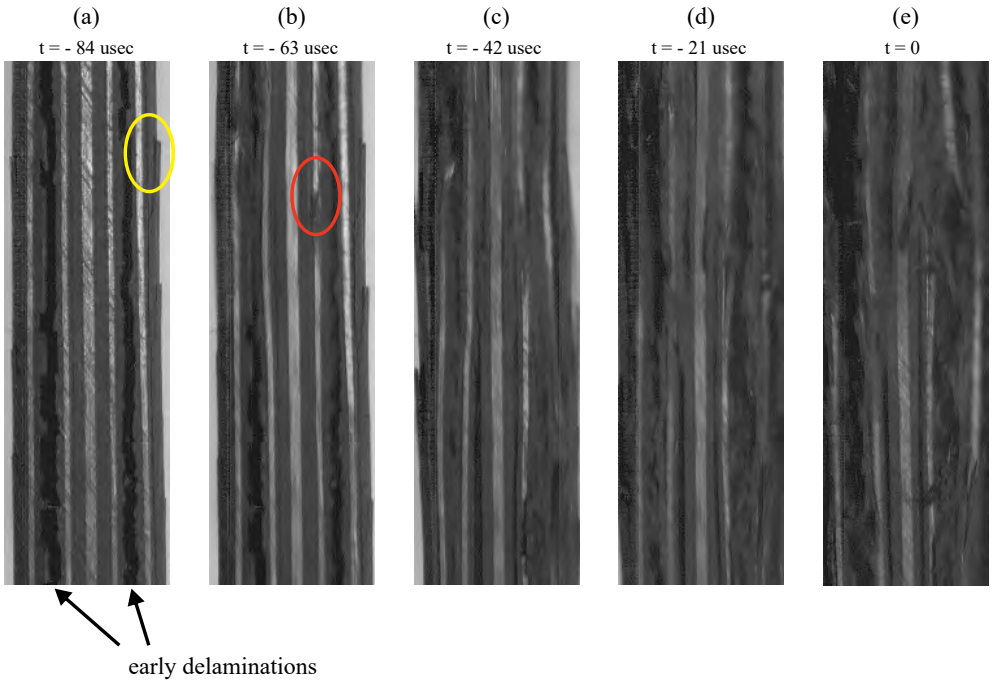

Figure 8: High speed camera frames: Tension test prior to final failure of pristine specimen 3, yellow and red ovals are indicating an early onset of surface ply damage and location of final failure initiation, respectively

b) Gaps

The frame series in Figure 9 has been obtained from the captured high speed camera pictures during the

tension test of a "Gap" specimen. In frame (a), the locations where the cross-over gaps reach the specimen's edge are indicated by the red squares. In addition, the frame (a) shows the premature damage in form of delaminations that occurred in each of the middle-most sub-laminate of the two symmetric parts. Similar to the pristine specimens, these delaminations are controlled by free edge failure, which occurred without any significant load drop in the force-displacement curve. In addition, the 45° surface plies tended to peel off, indicated by the yellow oval in frame (a). In Figure 9 (b), the red oval depicts the location where surface plies delaminated which triggered the catastrophic failure shown in frame (c). Figure 9 (d) and (e) depict the failure event further.

Differences between the pristine and the "Gap" failure mode may be seen in the space created by the early delaminations. The segregation of sub-laminates is more pronounced in the pristine specimens. However, no difference in the final failure mode compared with the pristine specimen was found (see Figure 8 for the pristine and Figure 9 for the "Gaps" specimen).

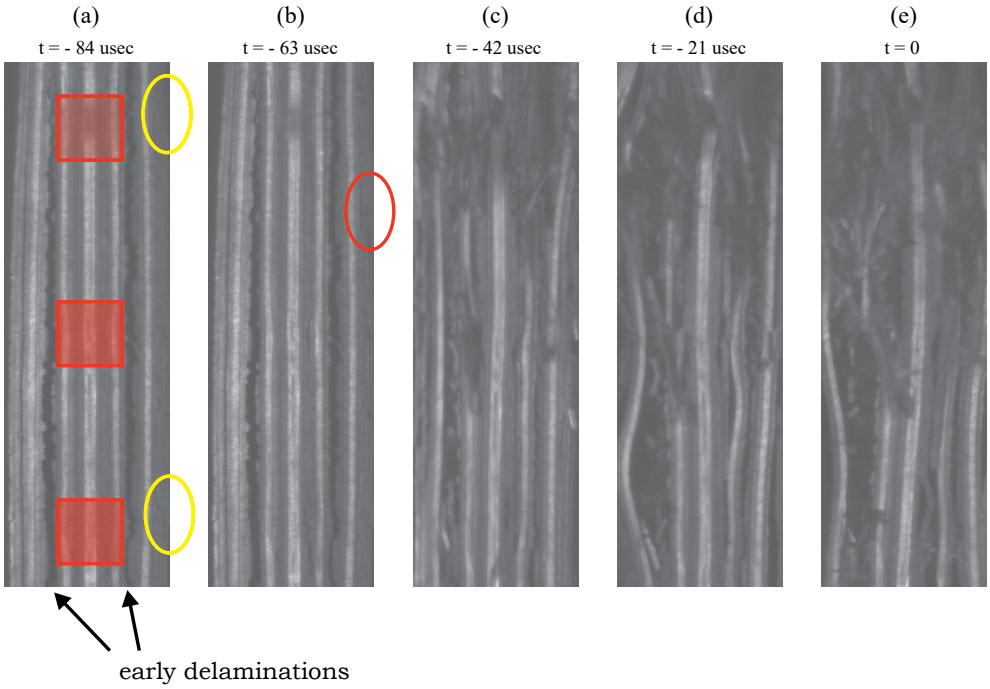

Figure 9: High speed camera frames: Tension test prior to final failure of "Gaps", specimen 1, the transparent red fields in frame (a) indicate the regions where the gaps reach the edge of the specimen, yellow and red ovals are indicating an early onset of surface ply damage and location of final failure initiation, respectively

c) Overlaps

Similar to the previous two specimen types, the "Overlaps" specimens revealed no obvious changes within the failure mode and the overall behaviour prior to catastrophic failure compared to the the pristine and

"Gaps" specimens. Surface ply splitting and early delaminations in the two middle-most sub-laminates were observed again that were followed by unstable crack growth that led to localised fibre failure. One aspect that can be clearly depicted from Figure 10 (a) is that the peeled off 45° surface plies cause initial delamination (regions indicated by the yellow ovals). The crack could propagate from the split ply into the interface between the ply itself and the adjacent 90° ply. Subsequently, the delamination grew into the next inner interface abetted by the transverse cracks in the 90° plies. At this location, however, the propagation is stopped and it can be assumed that the available energy at this point was not high enough in order to create new surfaces (Figure 10 (b)). Final failure occurred then by the breakage of a 0° ply (frame (c) in Figure 10). Figure 10 (d) and (e) depict the failure event further.

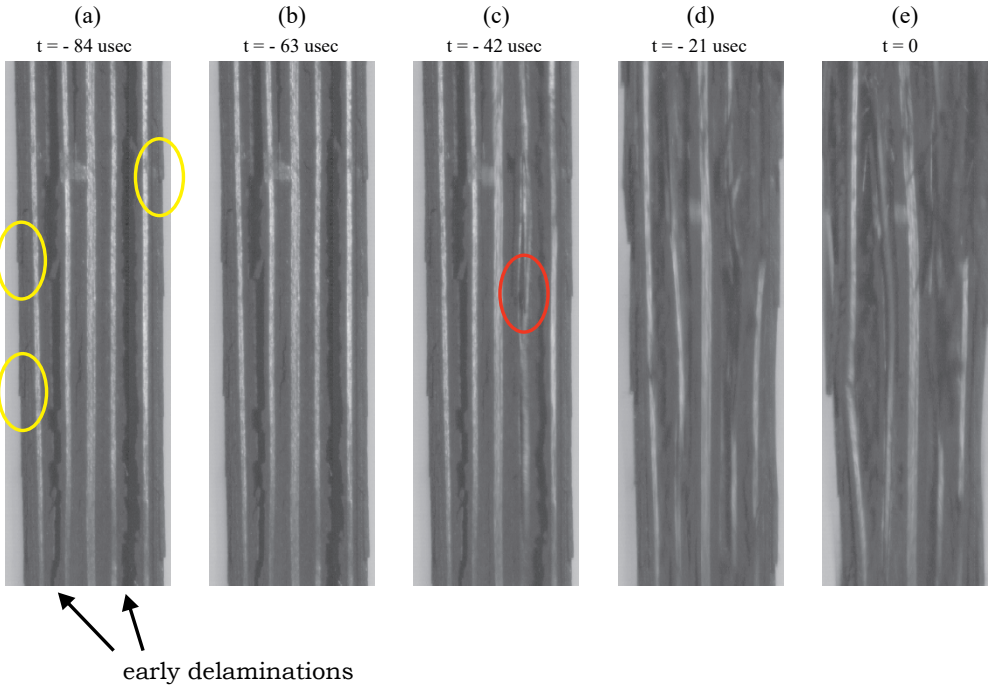

Figure 10: High speed camera frames: Tension test prior to final failure of "Overlaps" specimen 4, yellow and red ovals are indicating an early onset of surface ply damage and location of final failure initiation, respectively

d) Staggered Gaps

The manner in which the tension specimens of "Staggered Gaps" configuration failed is fairly similar to the specimens examined above. Matrix cracking accompanied by the peel off effect of the 45° surface plies were observed again (yellow oval in frame (a) in Figure 11). The cracking of the surface plies was followed by delaminations between internal off-axis plies. However, when looking at the HSC frames, shown in Figure 11, one can clearly see that the delamination size is smaller compared to the specimen types discussed before (see frames (a) and (b)). The occurrence of delaminations in the case of the "Staggered Gaps" specimens

was not limited to a few number of sub-laminates but could be observed in more interfaces. In addition, ply separations appeared less pronounced as it could be for example seen on the pristine specimens. In contrast to the previously discussed sample types, the initiation of the catastrophic failure caused by a breakage of 0° plies could not be observed for "Staggered Gaps" specimens. In the particular case of the specimen shown in Figure 11, final failure occurred as a result of unstable delamination propagation, which triggered a snap back motion prior to final failure. The red oval in frame (b) indicates the location of this motion. Figure 11 (c)-(e) depict the failure event further.

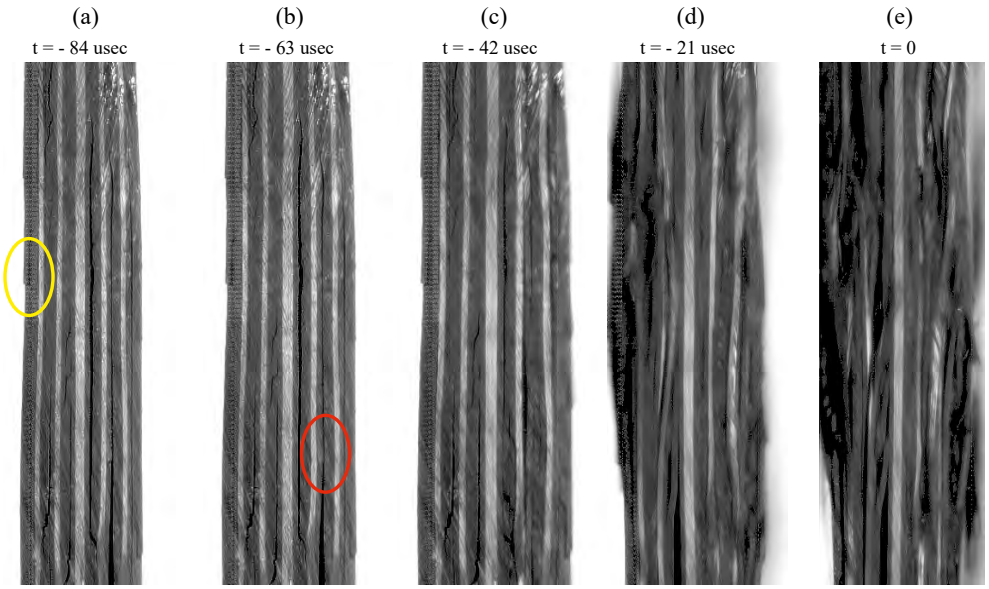

Figure 11: High speed camera frames: Tension test prior to final failure of "Staggered Gaps" specimen 3, yellow and red ovals are indicating an early onset of surface ply damage and location of final failure initiation, respectively

e) Gaps & Overlaps

The "Gaps & Overlaps" tension specimens (Figure 12) failed very similar to the specimens of "Staggered Gaps" (Figure 11). The most obvious difference was again the reduced level of the early delaminations. These delaminations seem to be more located around the defects compared to the pristine specimens where free edge delaminations along the entire gauge section were observed. Just small splittings within the specimens could be observed. However, the way in which the subsequent catastrophic failure has been initiated was similar compared with the "Staggered Gaps" specimens. The peel off effect on the specimen's surface are indicated by the yellow ovals in Figure 12 (a). Catastrophic failure occurred presumably due to unstable delamination propagation. The region, in which this propagation was evident is indicated by the red oval in frame (b). Figure 11 (c)-(e) depict the failure event further.

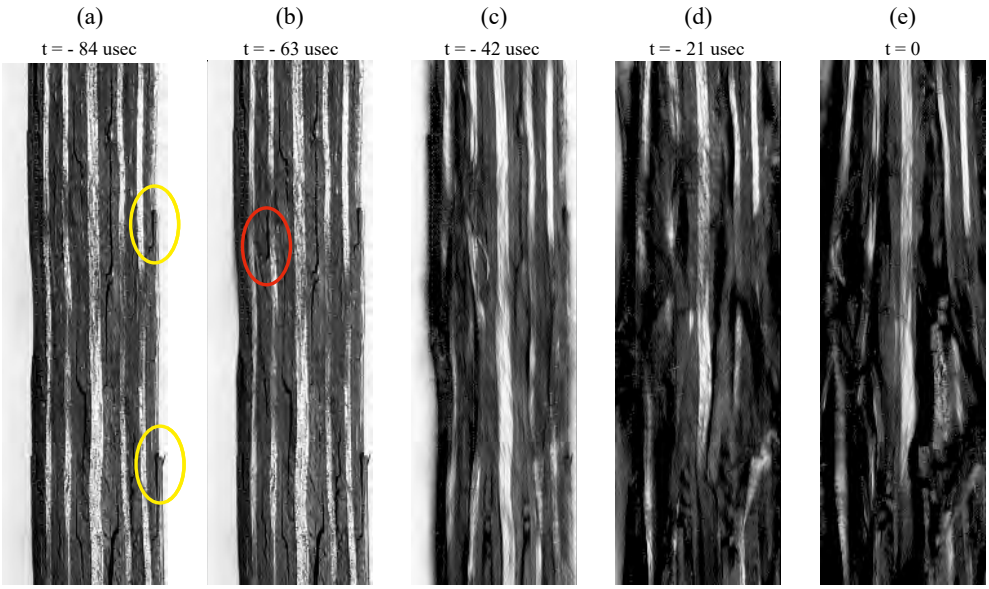

Figure 12: High speed camera frames: Tension test prior to final failure of "Gaps & Overlaps" specimen 2, yellow and red ovals are indicating an early onset of surface ply damage and location of final failure initiation, respectively

3.1.3. Discussion

The specimens tested in tension, independent of the defect configurations, exhibited free-edge delaminations prior to the final failure. This failure mode is constantly present since rather narrow specimens with free edges were tested. In principle, free edges are discontinuities in the layup which lead to the occurrence of high interlaminar stresses due to the change in elastic layer material properties. These stresses evoke reductions in the failure strength [13, 25]. Laminate edge treatments to alleviate the detrimental effect of free edges such as a progressive reduction of the fibre volume content towards the free edges [26] or an introduction of pure resin edges after composite curing [27] were not conducted in this study.

Despite the presence of the delamination failure mode, it seems that the defect configuration has an effect on the pattern of delaminations. It was found that the higher the amount of integrated defects the more localised the formation of free edge delamination. The pristine samples showed fairly large delamination zones, whereas the "Gaps" and "Overlaps" specimens exhibited a more localised damage pattern. The localisation of premature damage was found to be even more pronounced in the "Staggered Gaps" and "Gaps & Overlaps" samples. Cracks and minor delaminations at the position of the defects arose. It may be that the presence of the defects disrupts the major free edge delamination. Despite smaller delamination zones, observed in the two most significant defect configurations, the failure mode was still strongly influenced by delamination.

3.2. Compression testing

3.2.1. Strength and stiffness

The recorded stress-displacement curves of the compression specimens are shown in Figure 13. At least five curves per batch are illustrated, separated by an displacement offset of 1 mm to ease the comparison.

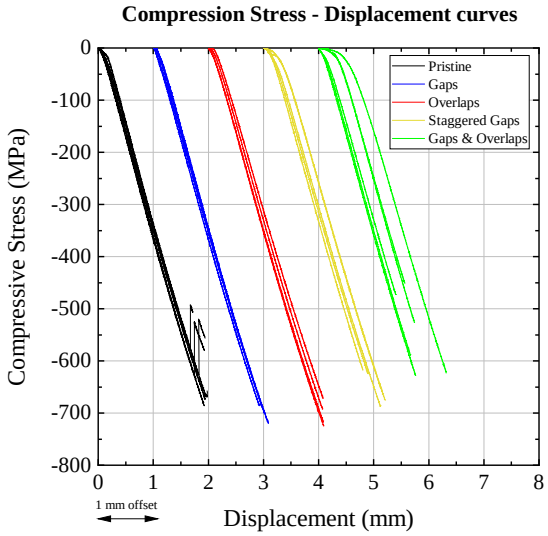

Figure 13: Compression stress-displacement curves (horizontal offset added for a better visualisation)

In Table 2, the measured compressive moduli, E_c, the average ultimate compressive failure strength values, $\bar{\sigma}_{c\,max}$, statistical numbers and knockdown factors of each defect configuration tested in compression are summarised. This table also contains the Student's t-test P-values and the interpretation of the statistical significance for the difference in failure strength. To account for potential low slopes of the curves at the beginning of compression tests, the strain range for the calculation of the compressive moduli were adapted to 0.2 – 0.4 %. Similar to the tensile specimens, a large change in the stiffness could not be recorded, suggesting that the material behaviour in the low strain regime is almost unaffected by the defects.

In terms of the strength, the pristine specimens reached an average compressive failure stress of 643 MPa. An interesting behaviour could be noticed on the pristine specimens which did not fail catastrophically after reaching the maximum load carrying ability, but were able to partially recover. The recovery is evident after the drops in the stress-displacement curves. The load did not go all the way down to zero but went to a certain level. From this level, the specimens were able to further increase their load bearing ability until final failure occurred in a catastrophic fashion. This effect is further analysed in conjunction with the failure behaviour in section 3.2.2. The "Gaps" specimens yielded an average strength value of 692 MPa, which is an increase of 7.6 %. The "Overlaps" specimens, similar to the tensile specimens, yielded the highest average ultimate failure strength value among the specimen types tested. The improvement compared

Table 2: Summary of *compressive* properties of pristine and of defect specimens and results of statistical significance based on Student's t-test

Configuration	n	E_c (GPa)	$\bar{\sigma}_{c\,max}$ (MPa)	CV of $\bar{\sigma}_{c\,max}$ (%)	Knockdown factor for $\bar{\sigma}_{c\,max}$ (%)	P-value	Significant difference in strength
Pristine	6	42.3 ± 0.8	-643 ± 40.6	6.31	–	–	–
Gaps	6	41.2 ± 0.7	-692 ± 16.3	2.35	-7.6	0.0087	yes
Overlaps	5	42.0 ± 1.2	-705 ± 21.7	3.08	-9.5	0.0173	yes
Staggered Gaps	5	42.3 ± 0.7	-652 ± 30.6	4.70	-1.3	0.9307	no
Gaps & Overlaps	6	39.7 ± 2.7	-549 ± 76.6	13.95	14.7	0.0411	yes

to the pristine properties is 9.5 %. The failure strength of the "Staggered Gaps" samples also showed a performance improvement of 1.3 %. The "Gaps & Overlaps" configuration finally yielded the more expected strength knockdown of 14.7 %. This knockdown value is beyond the scatter of the other samples types. A significant difference as the result of the Wilcoxon signed rank test are given for the "Gaps", "Overlaps" and "Gaps & Overlaps" specimens. However, it should be noted that only the "Gaps & Overlaps" specimens exhibit a positive knockdown factor.

3.2.2. Failure behaviour

a) Pristine

The final failure in compression of a carbon/epoxy specimen occurs suddenly without any significant sign compared for example with the peel-off effect of surface plies during a tensile test. However, in the case of the pristine specimens, a debonding effect could be observed. The compressive ply peel-off is caused by local buckling of several surface plies. In contrast, the peeling off during a tension test is primarily induced by matrix splitting [28]. The local buckling mode under uniaxial compression is reported in [29] as *buckle delamination* failure. This mode of failure occurs when surface layers are debonded from the main laminate, parallel to the loading direction. It may occur due to arising out-of-plane stresses, possibly as a result of fibre misalignment.

The high speed camera series in Figure 14 (a) shows that the first failure, i.e. buckling delamination, occurred on the right side of this particular specimen. This delamination was initiated in the centre of the gauge length and propagated towards the region close to the end tabs. The next failure event was the surface layer debonding on the left hand side of the specimen (indicated by the yellow oval in frame (b)). The development of this buckling related delamination is shown in the frames (b)-(f), which is closely followed by fibre failure (red oval in frame (g)), causing ultimate failure of the specimen. Figure 14 (h)-(j)

depict the failure event further.

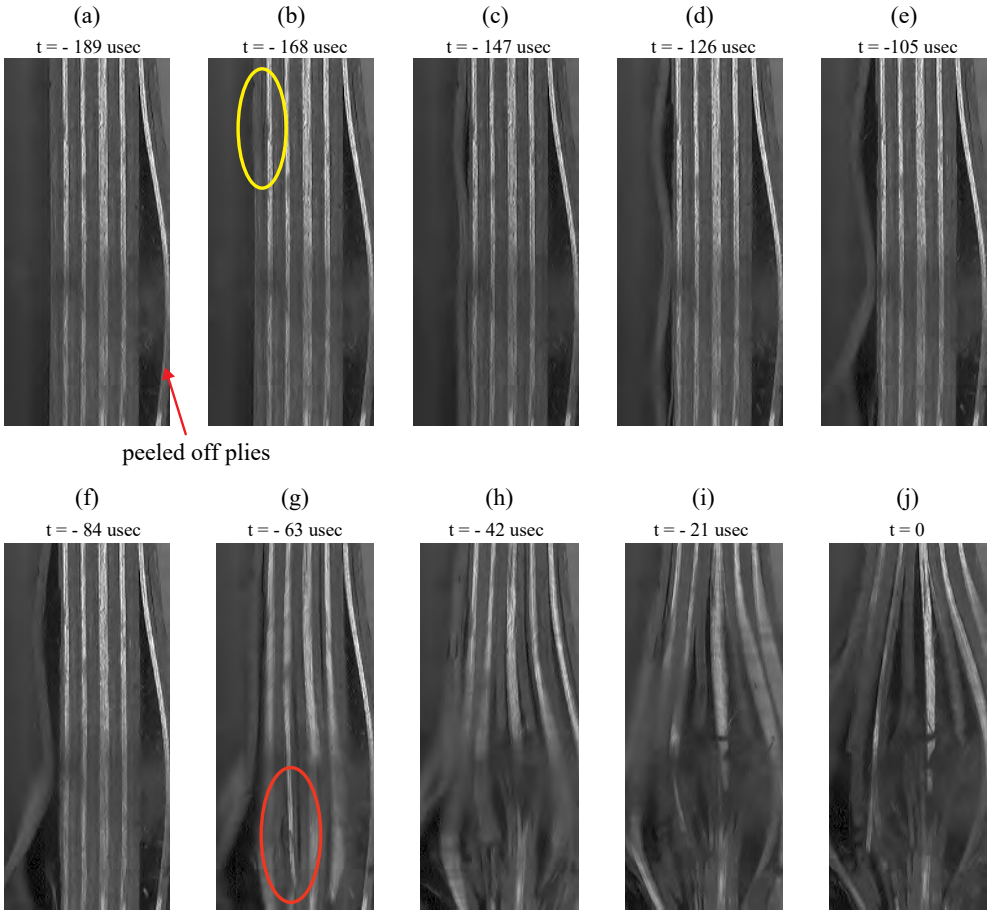

Figure 14: High speed camera frames: Compression test prior to final failure of pristine, specimen 4, yellow and red ovals are indicating the locations of failure initiation by delamination and fibre failure, respectively

An interesting phenomenon is the extensive peel-off effect associated with a significant drop in load but without a simultaneously occurring final failure. This effect could only be observed on pristine specimens tested in compression. After the sudden drop, the specimens still had the capability to carry almost the entire applied load. However, the load level, reached right before the significant load drop, could not be reached again. Thus, the maximum obtained load has been used for the calculation of the strength and its average value. Figure 15 shows a stress-displacement curve of a specimen that failed in such a manner described above. At the point of maximum load, some plies have been peeled off from one end of the specimen. The final failure, however, occurred accompanied by a similar effect, but on the opposite side of the specimen. Because of the debilitated structure as a result of these delamination failures, it can be assumed that the specimens ultimately failed by a combination of further delamination and fibre microbuckling or kinking [29].

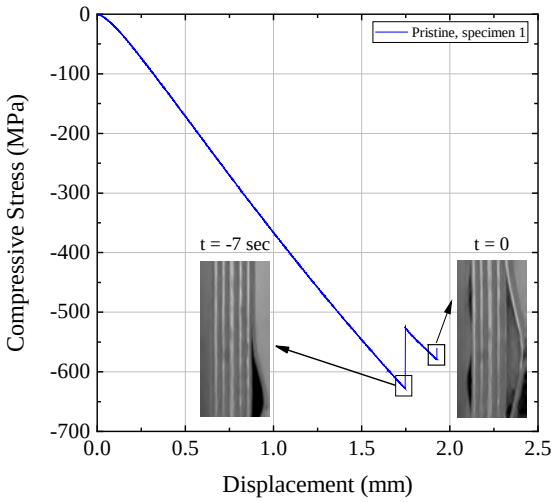

Figure 15: Compression stress-displacement chart with one-sided plies peel-off at maximum load without loosing integrity and subsequent final failure of a pristine specimen

The behaviour of the specimen shown in the stress-displacement diagram (Figure 15) is fairly similar to the one of specimen shown in the HSC images (Figure 14). However, this HSC specimen did not exhibit any significant drops in the recorded load. The final failure, based on the HSC analysis, occurred just 2.3 μs after the first buckle delamination. Thus, no obvious load drop was recorded. In general, it appears that the specimens can not retain their entire performance after the first significant damage occurs.

b) Gaps

The failure mode of the "Gaps" specimens cannot be precisely defined as a sequence of different interacting mechanisms led to the sudden failure (see Figure 16). One particular specimen (specimen no. 6) exhibited the peel off effect that could be seen on the pristine specimens. However, the significant load drop which was characteristic for the pristine specimens (Figure 15) was not observed. In addition, this premature failure (peel-off effect) was preceded by slight global buckling. Finally, the layer peel off was followed by simultaneous final fibre breakage associated with delaminations, which occurred especially in the 0/45 interfaces. As mentioned, this particular failure sequence could be observed just on one specimen of this set. Interestingly, this particular specimen yielded a slightly higher ultimate strength compared to the other "Gaps" specimens. The major failure mode, however, was a simultaneous appearance of 0/45 interface delaminations and localised fibre failure without early global buckling (see frame (b) in Figure 16). Since the difference in ultimate failure load of specimens exhibiting the slightly different damage mechanisms explained above is less than 3 %, we assume that the preceding buckling (observed just on one specimen) is a coupon alignment related issue.

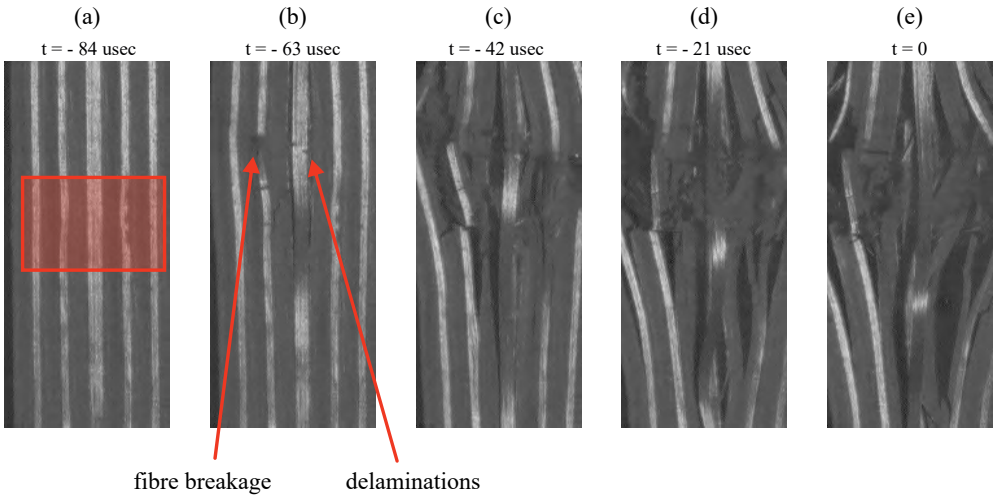

Figure 16: High speed camera frames: Compression test prior to final failure of "Gaps", specimen 8, the transparent red field in frame (a) indicates the region where the middle gap reaches the edge of the specimen

c) Overlaps

Similar to the "Gaps" coupons' failure modes, the "Overlaps" specimens also exhibited two different failure mode sequences. For the case that an early global buckling occurred, the subsequent final failure was a buckle delamination mode that occurred predominantly in 0/45 interfaces. In those cases in which no buckling preceded the major failure, the specimens failed by fibre breakage followed by complete delamination. Figure 17 shows the development of such a fracture behaviour. Frame (a) shows the intact specimens, whereas frame (b) the the fibre failure. The failure location is indicated by the red arrow. Figure 17 (c)-(e) depict the failure event further.

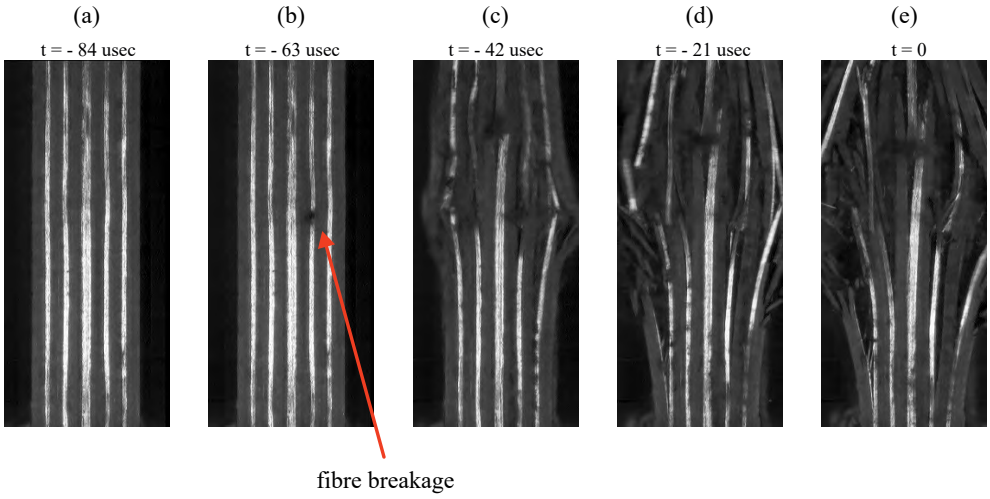

Figure 17: High speed camera frames: Compression test prior to final failure of "Overlaps", specimen 1

d) Staggered Gaps

The failure mode of the "Staggered Gaps" compression specimens was characterised by two types of failure sequences. Two specimens out of five tested failed by a preceding delamination initiation and subsequent loss of integrity, whereas the remaining three failed by fibre breakage and almost simultaneously triggered delamination. The latter failure sequence is shown in Figure 18. Frame (a) shows the intact specimen. In frame (b), the location of the fibre breakage is indicated by the red arrow. Form this damage location delamination could propagate towards both supports of the test jig. This event is shown in the frames (d)-(d). The failure stresses of this set of specimens correlate well with the corresponding damage mechanisms. The specimens that exhibited delaminations failed at loads above the pristine ultimate strength level, whereas the specimens that failed by fibre breakage failed at loads below the pristine level.

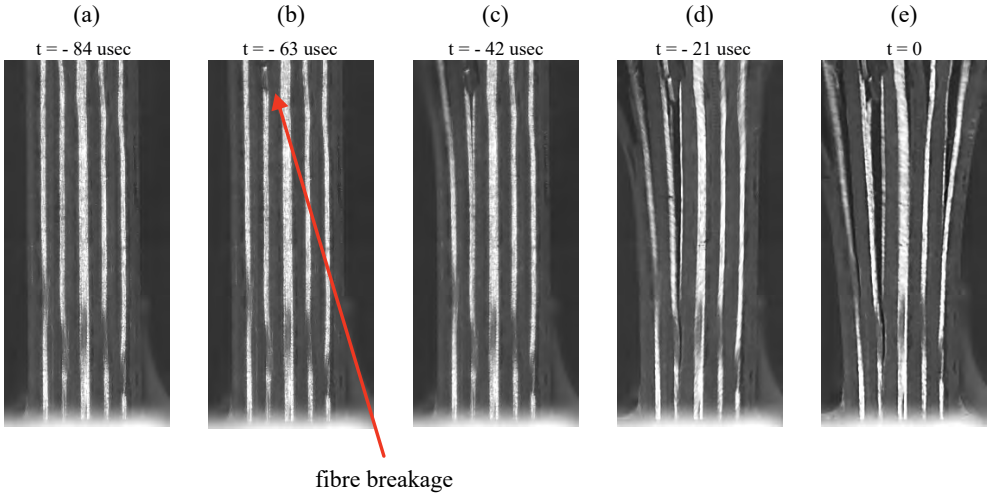

Figure 18: High speed camera frames: Compression test prior to final failure of "Staggered Gaps", specimen 1

e) Gaps & Overlaps

The compression specimens of "Gaps & Overlaps" failed by delamination without obvious premature fibre breakage. The red oval in frame (a) in Figure 19 indicates the location where delamination was initiated. Frame (b) depicts that fibre compression failure was observed at one edge of the specimen which occurred simultaneously with an opening mode of the delamination that arose shortly before the final failure event. The propagation of the delamination, which eventually led to fibre failure, is shown in frame (c). Figure 19 (d) and (e) depict the failure event further.

The comparatively high scatter with a coefficient of variation of almost 15 % in ultimate failure strength indicates a possible variation in the failure mode within this set of specimens. However, based on the high speed camera recordings, no obvious changes in failure mode were observed. This leads to the assumption that the reason for the high scatter may be found in the manufacturing process. Although all of the

specimens were extracted from the same composite panel, small local variations in terms of both quality (e.g. compaction) and thus properties, as well as the severity of fibre misalignments are possible.

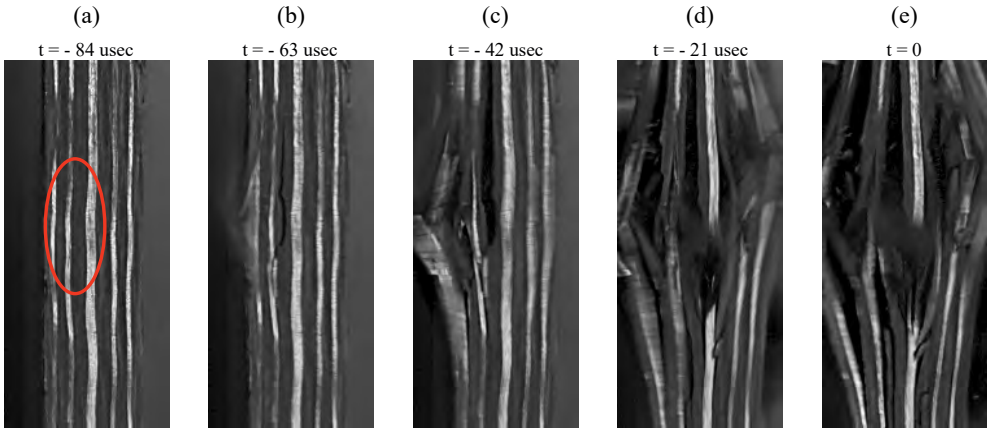

Figure 19: High speed camera frames: Compression test prior to final failure of "Gaps & Overlaps", specimen 3

3.2.3. Discussion

The pristine specimen failure is mainly characterised by premature delaminations caused by buckling of the sample. Two different pristine failure phenomena were observed. Failure occurred either suddenly without a significant load drop prior to the rapture, or with a drop in load associated with the debonding of one surface sub-laminate. The final failure, however, was always caused by fibre rapture. Similarly to the pristine samples, the "Gaps" and the "Overlaps" specimens failed by an axial overloading of the 0° plies, which was accompanied with a slight buckling. However, a premature debonding of sub-laminates could not be recorded for the "Gaps" and "Overlaps" specimens. When testing the specimens of the "Staggered Gaps" and "Gaps & Overlaps", a change in the failure sequence was noticed. In particular, the "Gaps & Overlaps" specimens showed initiation and evolution of delamination as well as matrix cracks prior to final failure (see frame (a) in Figure 19). Final failure was still caused by 0° fibre rapture. Although the "Staggered Gaps" configuration has also an elevated defect content, a distinct delamination failure that preceeds the final failure could not be observed. It is assumed that the severity of fibre misalignments controls the damage mechanisms rather than the actual amount of defects in the structure. Mukhopadhyay et al. [30] also pointed out this aspect. They studied the influence of out-of-plane fibre wrinkling on the compressive strength of carbon fibre/epoxy composites and found that the higher the severity of the fibre deviation, the higher the reduction in strength. Additionally, a transition from fibre dominated to a delamination failure mechanism was found, when the wrinkling severity was increased.

4. Summary and conclusions

In this work, different defect configurations that can arise in composite components that are manufactured by the Automated Fibre Placement (AFP) process were experimentally investigated. The overall goal was to get a better understanding of how defects affect the mechanical performance of composites. Therefore, gaps and overlap defect types were artificially introduced into carbon fibre/epoxy composite specimens. Defect formations to allow for significant reductions in the specimen's strength were developed via combinations of gaps and overlaps that cause fibre misalignments. The out-of-plane fibre misalignments cause interlaminar shear stresses and out-of-plane normal stresses that would promote an earlier occurrence of failure compared to the pristine specimens. Four defect configurations were developed, i.e. "Gaps", "Overlaps", "Staggered Gaps" and "Gaps & Overlaps". It was shown, via microscopy analysis, that the integration of 2 mm wide defects and 2 mm wide staggers can be precisely realised with the manufacturing method developed to simulate AFP defects by hand layup. The effects of gaps and overlaps in the developed defect configurations were studied under tension and compression testing.

The configurations "Gaps", "Overlaps" and "Staggered Gaps" did not yield a (positive) statistically significant knockdown in tensile or compressive strength. The "Gaps & Overlaps" specimens, however, exhibited the more expected strength reductions in tension and compression of 7.4 % and 14.7 %, respectively. Amongst the defect configurations considered in this study, the "Gaps & Overlaps" specimens were the only ones in which both gaps and overlaps defect types were combined. The results are consistent with other observations in the literature, e.g. those presented in [5], where isolated gaps and overlaps defects were shown to not cause a major knockdown in strength. A comparison of this work's knockdown factors with measures reported in the literature can be found in Table 3.

The failure behaviours of the defect specimens appear to be consistent with the level of ply waviness caused by the defects, which appears to be the main driving parameter. One should note that the measured knockdown factors are representative of the studied defect formations. Strength knockdowns for defects that occur during the actual industrial AFP process may be different. Based on the results presented here it can be postulated that if a defect in the AFP process is random, it is likely not to have a major detrimental effect. If however the defect is systemic, i.e. it occurs repeatedly and at the same location in each ply (or course) then the build-up of defects at the same location is likely to lead to a knockdown in material strength, compared to pristine properties.

In order to promote the understanding of effects of defects in laminated composites, further experiments along with numerical modelling should be carried out. For example, the defect configurations presented here could be extended in such a way that defect and stagger sizes along with ply width may be varied.

Table 3: Comparison of defect strength values and associated knockdown factors of this work with the literature

Reference	Test	Defect information	Baseline strength	Knockdown factor (%)
Croft et al. [5]	Tension	Gap	2268 MPa	2.12
		Overlap		-0.97
		half gap/overlap		3.40
	Compression	Gap	-1242 MPa	0.81
		Overlap		-7.17
		half gap/overlap		0
Sawicki and Minguet [3]	Compression	OL1*, 0.762 mm width	-	10 +
		OL1*, 2.54 mm width		14 +
		OL2, 0.762 mm width	-	10 +
		OL2, 2.54 mm width		9 +
Turoski [4]	Tension	3 gaps	982 MPa	15.60
	Compression	3 gaps	-544 MPa	8.50
This work	Tension	Gaps	750 MPa	1.3
		Overlaps		-3
		Staggered Gaps		0.2
		Gaps & Overlaps		7.4
	Compression	Gaps	-643 MPa	-7.6
		Overlaps		-9.5
		Staggered Gaps		-1.3
		Gaps & Overlaps		14.7

+ Knockdown values were extracted from the reference's figures as absolute numbers were not presented

Acknowledgements

The authors would like to acknowledge Rolls-Royce plc for the support of this research through the Composites University Technology Centre (UTC) at the University of Bristol (UK) and the UTC for Lightweight Structures and Materials and Robust Design at the Technische Universität Dresden (Germany).

References

[1] Chawla, K.K.. Composite Materials: Science and Engineering. SpringerLink : Bücher; Springer New York; 2012. ISBN 9780387743653.

[2] Lukaszewicz, D.H.J., Ward, C., Potter, K.D.. The engineering aspects of automated prepreg layup: History, present and future. Composites Part B: Engineering 2012;43(3):997–1009.

[3] Sawicki, A.J., Minguet, P.J.. The Effect of Intraply Overlaps and Gaps Upon the Compression Strength of Composite Laminates. In: AIAA/ASME/ASCE/SHS/ASC Structures, Structural Dynamics &Materials Conference. 1998, p. 744–754.

[4] Turoski, L.E.. Effects of Manufacturing Defects on the Strength of Toughened Carbon/Epoxy Prepreg Composites. Maser thesis; Montana State University - Bozeman; 2000.

[5] Croft, K., Lessard, L., Pasini, D., Hojjati, M., Chen, J., Yousefpour, A.. Experimental study of the effect of automated fiber placement induced defects on performance of composite laminates. Composites Part A: Applied Science and Manufacturing 2011;42(5):484–491.

[6] Li, X., Hallett, S.R., Wisnom, M.R.. Modelling the effect of gaps and overlaps in automated fibre placement (AFP)-manufactured laminates. Science and Engineering of Composite Materials 2015;22(2):115–129.

[7] Lan, M., Cartié, D., Davies, P., Baley, C.. Microstructure and tensile properties of carbon-epoxy laminates produced by automated fibre placement: Influence of a caul plate on the effects of gap and overlap embedded defects. Composites Part A: Applied Science and Manufacturing 2015;78:124–134.

[8] Lan, M., Cartié, D., Davies, P., Baley, C.. Influence of embedded gap and overlap fiber placement defects on the microstructure and shear and compression properties of carbon-epoxy laminates. Composites Part A: Applied Science and Manufacturing 2016;82:198–207.

[9] Li, X., Jones, M.I., Woigk, W., Hallett, S.R., Wisnom, M.R.. Modelling the effect of interacting gaps and overlaps in automated fibre placement (AFP) manufactured laminates. In: ECCM16 - 16th European Conference on Composite Materials, Seville, Spain. June; 2014, p. 22–26.

[10] Hsiao, H., Daniel, I.. Effect of fiber waviness on stiffness and strength reduction of unidirectional composites under compressive loading. Composites Science and Technology 1996;56(5):581–593.

[11] Potter, K.D.. Understanding the origins of defects and variability in composites manufacture. 17th International Conference on Composite Materials 2009;.

[12] Protz, R., Kosmann, N., Gude, M., Hufenbach, W., Schulte, K., Fiedler, B.. Voids and their effect on the strain rate dependent material properties and fatigue behaviour of non-crimp fabric composites materials. Composites Part B: Engineering 2015;83:346–351.

[13] Wisnom, M.R.. The role of delamination in failure of fibre-reinforced composites. Philosophical Transactions of the Royal Society A: Mathematical, Physical and Engineering Sciences 2012;370(1965):1850–1870.

[14] Hexcel, . Product Data Sheet - HexPly 8552; 2016.

[15] Haeberle, J.G., Matthews, F.L.. An improved technique for compression testing of unidirectional fibre-reinforced plastics; development and results. Composites 1994;25(5):358–371.

[16] Haeberle, J., Matthews, F.L.. Studies on compressive failure in unidirectional CFRP using improved test method. In: Developments in the Science and Technology of Composite Materials. 1990, p. 517–523.

[17] Lander, J.K., Kawashita, L.F., Allegri, G., Hallett, S.R., Wisnom, M.R.. A cut ply specimen for the determination of mixed-mode interlaminar fracture toughness. 14th European Conference on Composite Materials 2010;(June):1–11.

[18] Wisnom, M.R.; Khan, B.; Hallett, S.. Size eects in unnotched tensile strength of unidirectional and quasi-isotropic carbon_epoxy composites.pdf. Composite Structures 2008;84:21–28.

[19] Marlett, K.. Hexcel 8552 IM7 Unidirectional Prepreg 190 gsm & 35%RC Qualification Material Property Data Report. Tech. Rep.; 2011.

[20] Brewer, J.C., Lagace, P.a.. Quadratic Stress Criterion for Initiation of Delamination. Journal of Composite Materials 1988;22(12):1141–1155.

[21] Hallett, S.R., Jiang, W.G., Khan, B., Wisnom, M.R.. Modelling the interaction between matrix cracks and delamination damage in scaled quasi-isotropic specimens. Composites Science and Technology 2008;68(1):80–89.

[22] Wisnom, M.R., Hallett, S.R.. The role of delamination in strength, failure mechanism and hole size effect in open hole tensile tests on quasi-isotropic laminates. Composites Part A: Applied Science and Manufacturing 2009;40(4):335–342.

[23] ASTM International, . ASTM D3039 / D3039M - 14 - Standard Test Method for Tensile Properties of Polymer Matrix Composite Materials; 2014.

[24] Garrett, K.W., Bailey, J.E.. Multiple transverse fracture in 90 cross-ply laminates of a glass fibre-reinforced polyester. Journal of Materials Science 1977;12(1):157–168.

[25] Mittelstedt, C., Becker, W.. Free-Edge Effects in Composite Laminates. Applied Mechanics Reviews 2007;60(5):217.

[26] Shiau, L.C., Chue, Y.H.. Free-edge stress reduction through fiber volume fraction variation. Composite Structures 1991;19(2):145–165.

[27] Fletcher, T.A., Kim, T., Dodwell, T.J., Butler, R., Scheichl, R., Newley, R.. Resin treatment of free edges to aid certification of through thickness laminate strength. Composite Structures 2016;146:26–33.

[28] Hwang, S.F., Liu, G.H.. Buckling behavior of composite laminates with multiple delaminations under uniaxial compression. Composite Structures 2001;53(2):235–243.

[29] Budiansky, B., Fleck, N.. Compressive failure of fibre composites. Journal of the Mechanics and Physics of Solids 1993;41(1):183–211.

[30] Mukhopadhyay, S., Jones, M.I., Hallett, S.R.. Compressive failure of laminates containing an embedded wrinkle; Experimental and numerical study. Composites Part A: Applied Science and Manufacturing 2015;73:132–142.